

CGP37157, an inhibitor of the mitochondrial $\text{Na}^+/\text{Ca}^{2+}$ exchanger, protects neurons from excitotoxicity by blocking voltage-gated Ca^{2+} channels

A Ruiz^{1,2,3}, E Alberdi^{*,1,2,3} and C Matute^{*,1,2,3}

Inhibition of the mitochondrial $\text{Na}^+/\text{Ca}^{2+}$ exchanger (NCLX) by CGP37157 is protective in models of neuronal injury that involve disruption of intracellular Ca^{2+} homeostasis. However, the Ca^{2+} signaling pathways and stores underlying neuroprotection by that inhibitor are not well defined. In the present study, we analyzed how intracellular Ca^{2+} levels are modulated by CGP37157 (10 μM) during NMDA insults in primary cultures of rat cortical neurons. We initially assessed the presence of NCLX in mitochondria of cultured neurons by immunolabeling, and subsequently, we analyzed the effects of CGP37157 on neuronal Ca^{2+} homeostasis using cameleon-based mitochondrial Ca^{2+} and cytosolic Ca^{2+} ($[\text{Ca}^{2+}]_i$) live imaging. We observed that NCLX-driven mitochondrial Ca^{2+} exchange occurs in cortical neurons under basal conditions as CGP37157 induced a decrease in $[\text{Ca}^{2+}]_i$ concomitant with a Ca^{2+} accumulation inside the mitochondria. In turn, CGP37157 also inhibited mitochondrial Ca^{2+} efflux after the stimulation of acetylcholine receptors. In contrast, CGP37157 strongly prevented depolarization-induced $[\text{Ca}^{2+}]_i$ increase by blocking voltage-gated Ca^{2+} channels (VGCCs), whereas it did not induce depletion of ER Ca^{2+} stores. Moreover, mitochondrial Ca^{2+} overload was reduced as a consequence of diminished Ca^{2+} entry through VGCCs. The decrease in cytosolic and mitochondrial Ca^{2+} overload by CGP37157 resulted in a reduction of excitotoxic mitochondrial damage, characterized here by a reduction in mitochondrial membrane depolarization, oxidative stress and calpain activation. In summary, our results provide evidence that during excitotoxicity CGP37157 modulates cytosolic and mitochondrial Ca^{2+} dynamics that leads to attenuation of NMDA-induced mitochondrial dysfunction and neuronal cell death by blocking VGCCs.

Cell Death and Disease (2014) 5, e1156; doi:10.1038/cddis.2014.134; published online 10 April 2014

Subject Category: Neuroscience

Mitochondria regulate critical functions such as aerobic ATP production and cell survival by buffering cytosolic Ca^{2+} in physiological normal conditions. Conversely, mitochondrial dysfunction and Ca^{2+} overload occur in pathological conditions that involve a disruption of intracellular Ca^{2+} homeostasis, such as neurodegenerative disorders and ischemic injury.¹ Mitochondria modulate intracellular Ca^{2+} signaling with a complex toolkit for Ca^{2+} uptake and release recently characterized at the molecular level.² Thus, Ca^{2+} accumulation inside mitochondrial matrix, driven by the mitochondrial Ca^{2+} uniporter (MCU), is similar in most cell types, whereas excitable and non-excitable tissues may differ in Ca^{2+} efflux mechanisms.³ In neurons, mitochondrial Ca^{2+} is predominantly released by an $\text{Na}^+/\text{Ca}^{2+}$ exchanger (NCLX) that is Li^+ dependence,⁴ and it is specifically inhibited by the benzothiazepine CGP37157.^{5,6} Although it is well established that mitochondrial Ca^{2+} extrusion by NCLX contributes considerably to the control of Ca^{2+} -dependent functions, little is known about the relevance of its activity to

neuropathophysiology, and it remains controversial whether pharmacological inhibition of the exchanger attenuates tissue damage in ischemic or neurodegenerative conditions.⁷ Indeed, CGP37157 was shown to protect hippocampal slices against cytosolic Ca^{2+} and Na^+ overload⁸ whereas in a PINK-1-associated Parkinson's Disease model, inactivation of the mitochondrial $\text{Na}^+/\text{Ca}^{2+}$ exchanger contributed to mitochondrial Ca^{2+} overload and turned out to be detrimental.⁹

Overactivation of NMDA receptors (NMDARs) is considered to have a key role in glutamate-induced excitotoxicity in neurons of the CNS,¹⁰ and the underlying mechanism is dependent on (i) mitochondrial Ca^{2+} uptake,¹¹ which leads to mitochondrial dysfunction and cell death^{12,13} and (ii) cytosolic Ca^{2+} overload, which might trigger neuronal necrosis and apoptosis by the activation of calpains.¹⁴ In addition, Ca^{2+} elevations depolarize plasma membrane and open VGCCs that critically contribute to excitotoxicity.^{15,16} However, it is unclear whether inhibition of the NCLX by CGP37157 and its

¹Departamento de Neurociencias, Universidad del País Vasco-UPV/EHU, Barrio Sarriena s/n, Leioa, Spain; ²Achucarro Basque Center for Neuroscience-UPV/EHU, Zamudio, Spain and ³Instituto de Salud Carlos III, Centro de Investigación Biomédica en Red de Enfermedades Neurodegenerativas, (CIBERNED), Leioa, Spain
*Corresponding author: E Alberdi, Departamento de Neurociencias, Universidad del País Vasco, Barrio de Sarriena s/n, Leioa 48940, Spain. Tel: + 34 94 601 8280; Fax: + 34 94 601 3400; E-mail: elena.alberdi@ehu.es

or C Matute, Departamento de Neurociencias, Universidad del País Vasco, Barrio de Sarriena s/n, Leioa 48940, Spain. Tel: + 34 94 601 3244; Fax: + 34 94 601 3400; E-mail: carlos.matute@ehu.es

Keywords: CGP37157; NMDA receptor; mitochondrial Ca^{2+} ; neuronal excitotoxicity; NCLX

Abbreviations: NCLX, mitochondrial $\text{Na}^+/\text{Ca}^{2+}$ exchanger; CGP37157, 7-Chloro-5-(2-chlorophenyl)-1,5-dihydro-4,1-benzothiazepin-2(3H)-one; VGCC, voltage-gated calcium channel; NMDA, N-methyl-D-aspartate; ER, endoplasmic reticulum; SERCA, sarcoplasmic reticulum Ca^{2+} ATP-ase; RyR, ryanodine receptor; LDH, lactate dehydrogenase; ROS, reactive oxygen species

Received 29.11.13; revised 17.2.14; accepted 27.2.14; Edited by D Bano

associated signaling is neuroprotective. In this study, we have analyzed the effect of CGP37157 on NMDA-induced neuronal death and the mechanisms by which this NCLX inhibitor regulates cytosolic and mitochondrial Ca^{2+} signals during excitotoxicity *in vitro*. Our results show that benzothiazepine CGP37157 inhibits the mitochondrial $\text{Na}^+/\text{Ca}^{2+}$ exchanger in cortical neurons in basal conditions, and that it prevents from NMDA-induced cytosolic and mitochondrial Ca^{2+} overload and cell death by modulating Ca^{2+} entry through VGCCs.

Results

NCLX is expressed in cultured primary cortical neurons.

Previous reports have shown that NCLX is predominantly localized in the mitochondrial fraction of brain tissue as molecular forms of 50 and 70 kDa, together with an SDS-resistant 100 kDa dimer.⁴ In addition, the exchanger has been localized as well to the endoplasmic reticulum and plasma membrane¹⁷ and its expression and subcellular localization in different cell types of the central nervous system has not been analyzed so far. To determine whether NCLX is present in mitochondria in cultured primary cortical neurons, we carried out the immunolabeling of this exchanger in cells transfected with mitochondria-targeted DsRed (Figure 1a). Confocal microscopy analysis showed a positive staining for the NCLX (green) in cortical neurons which colocalizes with red mitochondria according to the fluorescence intensity analysis of the neuronal cross-section (Figure 1b) and overlap coefficient (0.78 ± 0.01 , $n = 32$ cells). Furthermore, immunoblotting analysis confirmed the expression of the 50 and 70 kDa forms of the mitochondrial $\text{Na}^+/\text{Ca}^{2+}$ exchanger in the neuronal cultures used in this study (Figure 1d), indicating that these cells express *in vitro* the NCLX protein described before in brain extracts.

CGP37157 inhibits mitochondrial $\text{Na}^+/\text{Ca}^{2+}$ exchanger in cortical neurons.

The benzothiazepine compound CGP37157 has been widely considered a specific inhibitor of mitochondrial $\text{Na}^+/\text{Ca}^{2+}$ exchanger (at $10 \mu\text{M}$ or below) in several cell types,^{6,18} but its specificity remains controversial. CGP37157 was shown to regulate VGCCs in dorsal root ganglion neurons¹⁹ and pancreatic β cells²⁰ whereas in these cells a selective inhibition of NCLX *in vivo* and *in vitro* was previously demonstrated.²¹ In addition, CGP37157 was also described to induce ER Ca^{2+} depletion by ryanodine receptor activation and to inhibit the endoplasmic reticulum Ca^{2+} ATP-ase (SERCA) in skeletal and cardiac muscle.²² To assess the effects of CGP37157 on mitochondrial Ca^{2+} homeostasis, cortical neurons were transfected with the genetically encoded Ca^{2+} indicator 2mtD4cpv (Figure 2a) and FRET signal recorded by single cell confocal imaging. Addition of CGP37157 caused a slow accumulation of mitochondrial Ca^{2+} that reached a $115.7 \pm 2.2\%$ ($n = 23$) of baseline levels (100%) after 10 min (Figure 2b). Treatment of neurons with CGP37157 for 1 h increased the mitochondrial Ca^{2+} levels to $137.5 \pm 7.8\%$ ($n = 94$) compared with control (untreated cells, 100%, $n = 112$) (Figure 2c). Concomitantly with this mitochondrial Ca^{2+} ($[\text{Ca}^{2+}]_{\text{mit}}$) increase, intracellular Ca^{2+} levels ($[\text{Ca}^{2+}]_{\text{i}}$) fell rapidly to a 90% ($n = 51$) compared with resting Ca^{2+} levels (100%), as observed in

Fluo-4 AM-loaded neurons (Figure 2d). On the other hand, cytosolic Na^+ levels ($[\text{Na}^+]_{\text{i}}$) reached a $117.7 \pm 1.7\%$ ($n = 86$) of basal content (100%) during 10 min after addition of CGP37157 in neurons loaded with sodium green fluorescent dye (Figure 2e). Application of 1 mM of acetylcholine (ACh) to neurons was used to analyze whether NCLX conducts mitochondrial Ca^{2+} efflux. Agonist caused mitochondrial Ca^{2+} transients characterized by a fast initial influx resulting in an increase of $131.1 \pm 3.2\%$ ($n = 33$) of resting Ca^{2+} levels that was followed by an efflux (at a rate of $130 \pm 24 \times 10^{-3}/\text{s}$) during exposure to the agonist (Figures 2f and g). Stimulation of acetylcholine receptors in the presence of CGP37157 prevented Ca^{2+} efflux (rate $-2.8 \pm 8.5 \times 10^{-3}/\text{s}$, $n = 30$) (Figures 2f-h). Interestingly, acetylcholine-induced $[\text{Ca}^{2+}]_{\text{mit}}$ increase was also reduced by CGP37157 to $117.3 \pm 1.8\%$ suggesting that it may modulate Ca^{2+} entry as well from the extracellular space (Figures 2f and g).

CGP37157 modulates intracellular Ca^{2+} levels through the inhibition of voltage-gated calcium channels.

CGP37157 may cause blockade of cell Ca^{2+} entry by Ca^{2+} channels in high K^+ -depolarized SH-SY5Y cells.²³ Therefore, we examined whether CGP37157 modulates VGCCs in depolarization-induced neuronal Ca^{2+} currents in both cytosol and mitochondria of cortical neurons. Application of KCl (50 mM, 10 min) induced a fast $[\text{Ca}^{2+}]_{\text{i}}$ increase with a peak amplitude of $293.1 \pm 14\%$ ($n = 58$) compared with resting levels (100%) that was reduced in a dose-dependent manner by 10 and $50 \mu\text{M}$ nifedipine to $222.2 \pm 7.3\%$ ($n = 89$) and $184.9 \pm 6\%$ ($n = 70$), respectively (Figure 3a). Similarly, the $[\text{Ca}^{2+}]_{\text{i}}$ increase induced by KCl was reduced by CGP37157 (peak amplitude of $199.8 \pm 6.5\%$; $n = 84$) (Figure 3a). Moreover, we observed that CGP37157 reduced the depolarization-induced $[\text{Ca}^{2+}]_{\text{mit}}$ increase in neurons transfected with the mitochondria-targeted cameleon. Thus, KCl provoked a mitochondrial Ca^{2+} accumulation (peak amplitude of $153.9 \pm 4.6\%$; $n = 22$) compared with resting levels (100%) after 10 min stimulation that was robustly reduced by CGP37157 (peak amplitude of $120.3 \pm 3.2\%$; $n = 31$) (Figure 3b). Finally, we analyzed whether CGP37157 induced ER Ca^{2+} depletion either in the long term, presumably by preventing store-refilling, or by inducing Ca^{2+} release through ryanodine receptors. First, $10 \mu\text{M}$ of CGP37157 was added to neurons in the absence of extracellular Ca^{2+} and no $[\text{Ca}^{2+}]_{\text{i}}$ increase was observed, whereas thapsigargin, an inhibitor of the ER SERCA pump, swiftly increased the $[\text{Ca}^{2+}]_{\text{i}}$ to $181 \pm 13\%$ ($n = 86$) of basal Ca^{2+} content (100%) (Figure 3c). To determine whether CGP37157 could contribute to depleting or preventing the refilling of intracellular stores, thapsigargin-induced $[\text{Ca}^{2+}]_{\text{i}}$ increases were compared in control neurons and in neurons pre-incubated with CGP37157. We found no significant differences in the peak responses ($127.9 \pm 2.9\%$, $n = 85$, and $130.9 \pm 3\%$, $n = 80$, respectively) (Figure 3d). Taken together, these results indicate that CGP37157 blocks both NCLX and VGCCs in neurons whereas it does not contribute to depletion of ER Ca^{2+} stores.

NMDA-induced cytosolic and mitochondrial Ca^{2+} overloads are reduced by CGP37157. Selective inhibition of NCLX by CGP37157 results in increased $[\text{Ca}^{2+}]_{\text{mit}}$ after

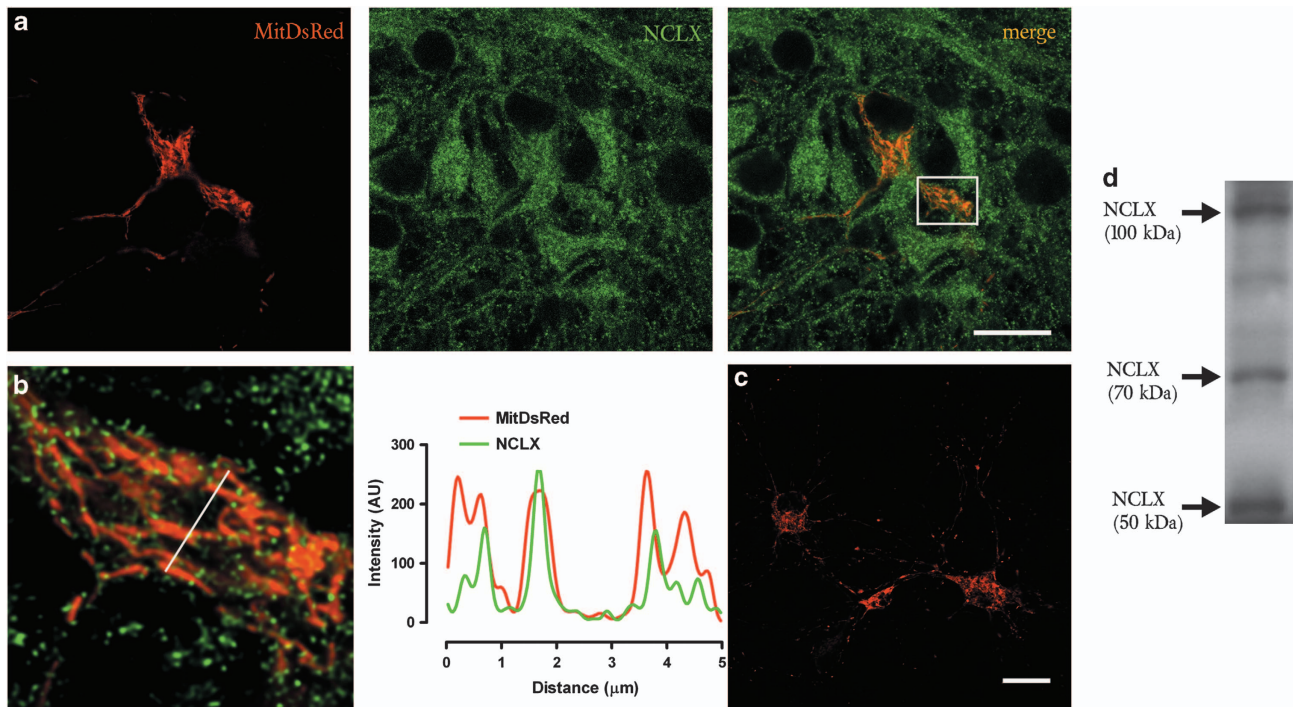


Figure 1 NCLX is expressed in cortical neurons *in vitro*. (a) Primary neurons expressing mitochondria-targeted DsRed were stained with rabbit anti-NCLX antibody. Colocalization of the exchanger (green) and mitochondrial red protein is shown in merged image. Scale bar: 20 μm . (b) Deconvolution and zoom of the selected field showing colocalization of NCLX (green) and mitochondria (red) and the fluorescence intensity plot of the cross-section (bottom); Y axis: fluorescence intensity (arbitrary units). X axis: distance (μm). (c) Immunolabeling without NCLX antibody showed no green staining (d) Immunoblot analysis of NCLX of total cell lysate from cultured cortical neurons

ATP-mediated intracellular Ca^{2+} release in astrocytes.²⁴ In neurons, activation of NMDA receptors results in a privileged Ca^{2+} access to mitochondria.²⁵ To analyze whether CGP37157 modulates mitochondrial Ca^{2+} homeostasis during NMDA receptor-mediated excitotoxicity, neurons were stimulated with NMDA in the presence of the $\text{Na}^+/\text{Ca}^{2+}$ exchanger blocker and $[\text{Ca}^{2+}]_{\text{mit}}$ measured by the mitochondria-targeted Ca^{2+} indicator. In control cells, NMDA (30 μM , 5 min) led to a maximum $[\text{Ca}^{2+}]_{\text{mit}}$ increase of $198.3 \pm 6.6\%$ ($n=33$) compared with resting Ca^{2+} levels (100%) (Figure 4a). Interestingly, in neurons pre-incubated with CGP37157, $[\text{Ca}^{2+}]_{\text{mit}}$ increase was strongly reduced to $150.9 \pm 4.9\%$ ($n=42$) (Figure 4a). As CGP37157 reduced the depolarization-induced (evoked by high K^+) $[\text{Ca}^{2+}]_{\text{mit}}$ and $[\text{Ca}^{2+}]_{\text{i}}$ increases, we next analyzed whether VGCCs contributed the NMDA-induced mitochondrial Ca^{2+} overload in this preparation. As expected, nifedipine (10 μM , 30 min) inhibited the $[\text{Ca}^{2+}]_{\text{mit}}$ increase after NMDA application to $161.3 \pm 4.9\%$ ($n=41$) (Figure 4a).

To verify that the effect of CGP37157 on mitochondrial Ca^{2+} signals was not due to the inhibition of a reverse NCLX activity during NMDA receptor activation, $[\text{Na}^+]_{\text{i}}$ was measured in the same experimental conditions. In control cells, NMDA (30 μM) induced a $[\text{Na}^+]_{\text{i}}$ increase of $127 \pm 1.6\%$ (peak amplitude, $n=99$) of resting levels (100%) which was reduced in the presence of CGP37157 to $112.5 \pm 1.69\%$ (peak amplitude, $n=83$). Nifedipine also attenuated NMDA-induced $[\text{Na}^+]_{\text{i}}$ increase from $137.3 \pm 2.7\%$ to $126.2 \pm 1.5\%$ of basal levels (100%) (peak amplitude, $n=68$) (Figure 4b). These results suggested that the effect of CGP37157 on $[\text{Ca}^{2+}]_{\text{mit}}$

during excitotoxicity relies on the modulation of the Ca^{2+} entry from the extracellular space more than in the modulation of the NCLX activity. To confirm this hypothesis, we next tested whether CGP37157 attenuated the depolarization-induced cytosolic Ca^{2+} load during NMDA stimuli in neurons. Neurons were loaded with Fluo-4 and the NMDA-induced $[\text{Ca}^{2+}]_{\text{i}}$ increase was measured in the presence of CGP37157 or the VGCC inhibitor nifedipine. NMDA alone triggered a $[\text{Ca}^{2+}]_{\text{i}}$ increase of $263.3 \pm 7.9\%$ ($n=91$) compared with resting levels (100%), which was significantly reduced by nifedipine to $191.8 \pm 7.3\%$ ($n=68$), indicating that VGCCs contribute to NMDA-induced $[\text{Ca}^{2+}]_{\text{i}}$ overload (Figure 4c). Similarly to nifedipine, CGP37157 reduced the $[\text{Ca}^{2+}]_{\text{i}}$ increase to $188.8 \pm 5.6\%$ ($n=102$) after the application of NMDA (Figure 4c).

Thus, these results suggest that CGP37157 shapes cytosolic and mitochondrial Ca^{2+} signaling during excitotoxicity by modulating VGCCs rather than through a selective inhibition of the mitochondrial $\text{Na}^+/\text{Ca}^{2+}$ exchanger.

CGP37157 reduces NMDA-induced excitotoxicity by the attenuation of mitochondrial damage and calpain activity in neurons. Mitochondrial Ca^{2+} uptake is a critical step for NMDA receptor-mediated glutamate excitotoxicity,¹¹ whereas mitochondrial $\text{Na}^+/\text{Ca}^{2+}$ exchanger inhibitor CGP37157 turned out to be neuroprotective in several models of Ca^{2+} overload.²³ To study the effect of CGP37157 on NMDA-induced excitotoxicity, primary cultures of cortical neurons were exposed to the drug before and during application of NMDA (30 and 100 μM) and LDH

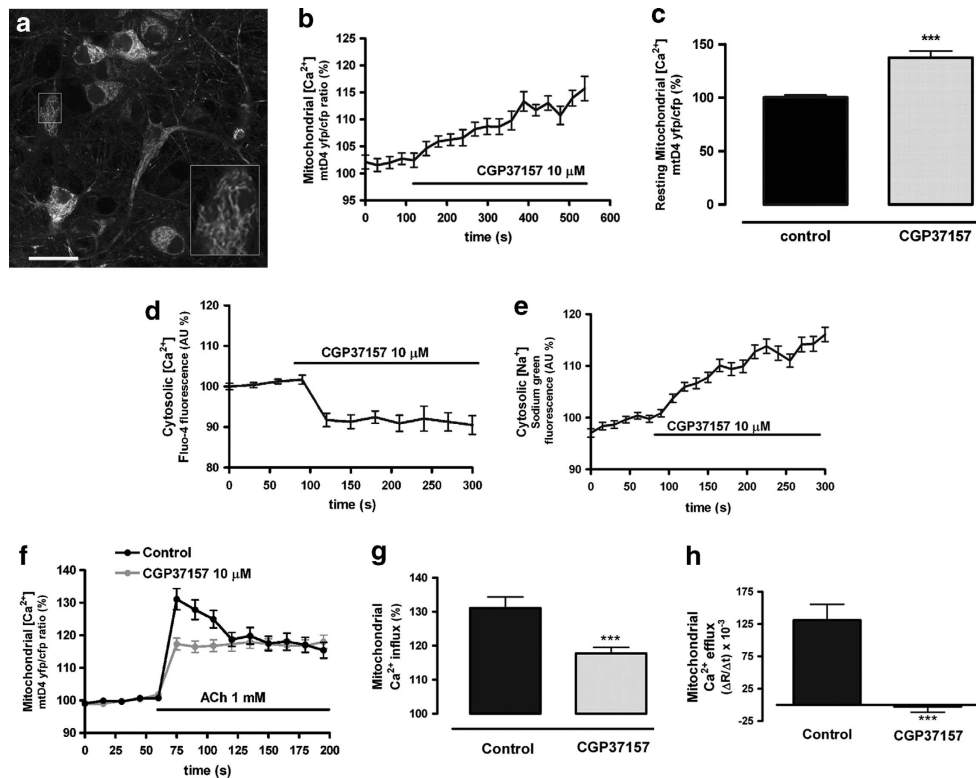


Figure 2 Mitochondrial $\text{Na}^+/\text{Ca}^{2+}$ exchange is inhibited by CGP37157 in cultured neurons. (a–c) CGP37157 ($10\ \mu\text{M}$) induces an accumulation of Ca^{2+} in mitochondria of neurons. Cells were transfected with the genetically encoded Ca^{2+} indicator 2mtD4cpv at DIV0 (a), and $[\text{Ca}^{2+}]_{\text{mit}}$ recorded after 8–10 days in culture (a). Scale bar: $20\ \mu\text{m}$. CGP37157 causes a steady increase in mitochondrial $[\text{Ca}^{2+}]$ levels ($n=23$) (b), which are robust after 1 h of pre-incubation with the drug ($n=94$) (c). Normalized average \pm S.E.M. of the yfp/cfp ratios are shown. $***P < 0.001$ compared with untreated cells; Student's *t*-test. (d, e) Neurons were loaded with Fluo-4 or Sodium Green fluorescence dyes and cytosolic $[\text{Ca}^{2+}]$ and $[\text{Na}^+]$ changes measured upon addition of CGP37157 $10\ \mu\text{M}$ ($n=51$ and $n=86$, respectively). (f–h) CGP37157 blocks mitochondrial Ca^{2+} efflux in neurons. (f) Mitochondrial $[\text{Ca}^{2+}]$ changes were monitored in control ($n=33$) and CGP37157-treated ($n=30$) neurons during stimulations with acetylcholine ($1\ \text{mM}$). Traces represent the time course of normalized yfp/cfp average ratios \pm S.E.M. of cells from at least three independent culture/experiments. (g and h) Statistical analysis was carried out according to influx and efflux rates, which are represented as the average \pm S.E.M. of maximal amplitudes and slopes of recorded single neurons, respectively. $***P < 0.001$ compared with untreated cells; Student's *t*-test

release to the medium was quantified 24 h later. We observed a dose-dependent LDH release of $257.5 \pm 16.1\%$ at NMDA $30\ \mu\text{M}$ ($n=7$) and $404 \pm 40.9\%$ at NMDA $100\ \mu\text{M}$ ($n=7$) compared with control (untreated cells, 100%) that was significantly reduced by CGP37157 to $199.6 \pm 7.4\%$ and $338.5 \pm 15.2\%$, respectively (Figure 5a). To verify whether VGCCs contributed to the NMDA-induced toxicity, neurons were exposed to $30\ \mu\text{M}$ of NMDA in the presence of nifedipine ($10\ \mu\text{M}$) which attenuated LDH release from $224.6 \pm 33.7\%$ to $184.4 \pm 33.7\%$ ($n=6$) (Figure 5b). Simultaneous incubation of neurons with nifedipine and CGP37157 did not reduce LDH release further ($161.7 \pm 26.1\%$, $n=6$, nonsignificant *versus* each drug alone) (Figure 5c).

We had previously shown that NMDA-mediated toxicity involves mitochondrial membrane depolarization and generation of reactive oxygen species (ROS).²⁶ Thus, we analyzed whether CGP37157 modulated NMDA-induced mitochondrial damage, as a consequence of the regulation of mitochondrial Ca^{2+} uptake during excitotoxicity. To measure the oxidative stress, cells were loaded with CM-H2DCFDA and ROS-induced fluorescence signal was quantified in $100\ \mu\text{M}$ NMDA-treated neuronal cells. Excitotoxic stimuli increased ROS up to $142.1 \pm 15.6\%$ ($n=4$) compared with untreated cells (100%) whereas the pre-incubation with CGP37157 reduced the

generation of ROS by 52% (to $120.5 \pm 11.2\%$ of control; Figure 5c). Next, we analyzed the effect of the NCLX inhibitor on mitochondrial membrane potential during excitotoxicity. Neurons were exposed to NMDA ($100\ \mu\text{M}$, 10 min) and the mitochondrial depolarization measured 45 min later by the fluorescent dye JC-1. NMDA induced a $13.8 \pm 1.3\%$ depolarization (to 86.1% of untreated cells 100%, $n=4$), which was attenuated by 50.7% in the presence of CGP37157 (to $92.9 \pm 2.9\%$ of control, $n=4$; Figure 5d). Finally, to analyze whether CGP37157 regulates excitotoxic apoptosis we studied the activation/cleavage of caspase-3 in NMDA-stimulated neurons when the NCLX inhibitor was present. NMDA ($30\ \mu\text{M}$, 30 min) triggered cleavage of pro-caspase-3 and production of a 29 kDa fragment (Figure 5e) previously identified as a calpain-produced caspase-3 intermediate.^{27,28} In contrast to NMDA, staurosporine cleaved the caspase-3 proform to produce a 17 kDa fragment, as well as the caspase-3 specific target Poly-ADP-ribose polymerase (PARP) (Figure 5f), revealing different signaling pathways activated by each drug. In the presence of CGP37157, however, the NMDA-induced and calpain-mediated caspase-3 cleavage was diminished to $24.1 \pm 14.8\%$ ($n=4$) of control (NMDA alone, 100%). In turn, since inhibition of VGCCs was previously shown to attenuate the apoptotic cascade in rat hippocampus

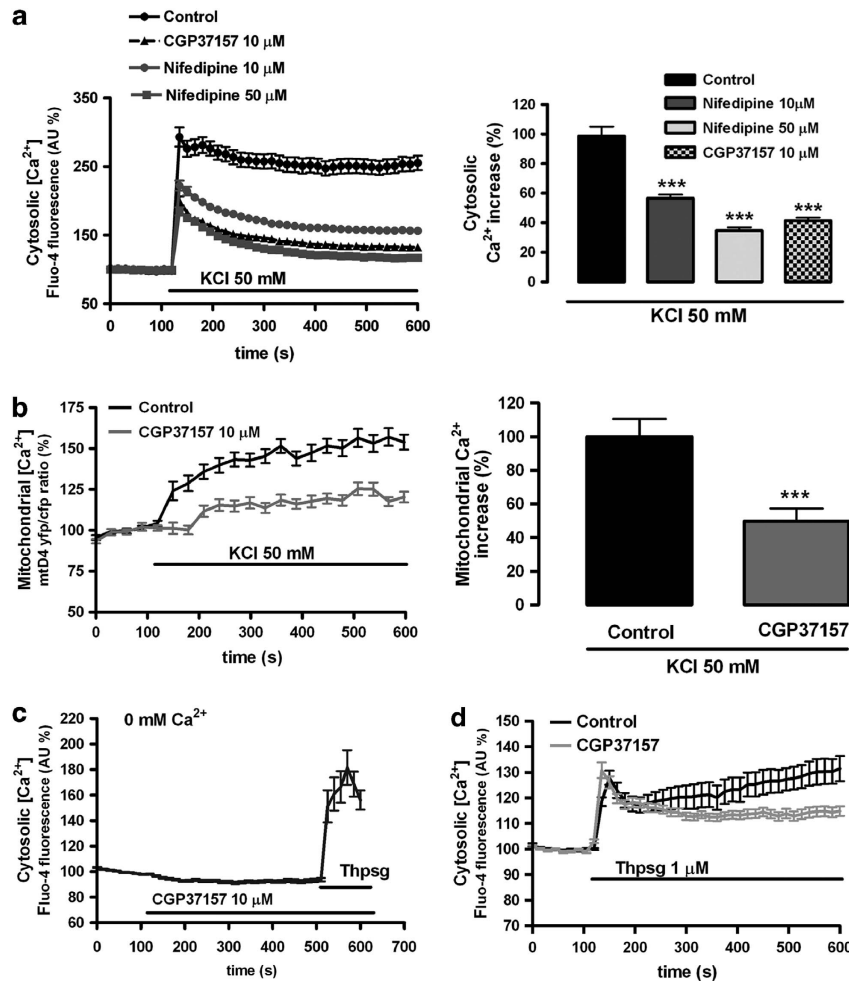


Figure 3 Neuronal VGCCs but not ER Ca^{2+} stores are modulated by CGP37157. (a) Depolarization-induced cytosolic Ca^{2+} increase is reduced by CGP37157. Fluo-4-loaded neurons were exposed to 50 mM of KCl ($n = 58$) in the presence of CGP37157 ($10 \mu\text{M}$, 1 h, $n = 84$) or nifedipine (10 and $50 \mu\text{M}$, 30 min, $n = 89$ and 70 , respectively) and cytosolic Ca^{2+} loads quantified. Traces represent normalized single-cell fluorescence intensity means \pm S.E.M. from at least three independent cultures/experiments. For statistical analysis normalized average \pm S.E.M. of the area under curve was calculated. $***P < 0.001$ compared with control cells; Student's *t*-test. (b) Depolarization-induced mitochondrial Ca^{2+} increase is reduced by CGP37157. Neurons transfected with the mitochondria-targeted Ca^{2+} sensor were stimulated with 50 mM of KCl ($n = 22$) as indicated and the effect of CGP37157 ($10 \mu\text{M}$, 1 h, $n = 31$) was monitored. For statistical analysis of the mitochondrial Ca^{2+} increase, the average \pm S.E.M. of the area under curve was calculated. $***P < 0.001$ compared with control cells; Student's *t*-test. (c and d) CGP37157 does not induce ER Ca^{2+} depletion. (c) Fluo-4-loaded neurons ($n = 86$) were exposed to CGP37157 ($10 \mu\text{M}$, 380 s) in the absence of extracellular Ca^{2+} and finally stimulated with thapsigargin ($1 \mu\text{M}$, 100 s) as positive control of ER Ca^{2+} release. Traces represent normalized average \pm S.E.M. of at least three independent experiments. (d) Fluo-4-loaded neurons were exposed to thapsigargin ($1 \mu\text{M}$) in the absence ($n = 85$) or presence of CGP37157 ($10 \mu\text{M}$, 1 h, $n = 80$) and the time courses of the evoked cytosolic Ca^{2+} increases were monitored. Traces represent $[\text{Ca}^{2+}]_i$ changes (mean \pm S.E.M.) of at least three independent experiments

during ischemia,²⁹ we tested whether nifedipine alone was able to decrease the calpain-mediated caspase-3 cleavage in our excitotoxic model. Consistent with toxicity data, nifedipine reduced cleaved/pro-caspase-3 ratio to $59.9 \pm 10.9\%$ ($n = 4$) of control (100%). Thus, these results indicate that CGP37157 might protect neurons from NMDA-induced mitochondrial damage and calpain activity by modulating VGCCs.

Discussion

The NCLX inhibitor CGP37157 is neuroprotective⁸ and modulates cytosolic Ca^{2+} signaling³⁰ in hippocampal slices. However, most studies describing the effects of CGP37157 during a neuronal Ca^{2+} dyshomeostasis were based on the analysis of $[\text{Ca}^{2+}]_i$, and whether NCLX inhibition contributes

to neuroprotection in the experimental conditions assayed remains controversial. In this study, we demonstrate that CGP37157 inhibits the NCLX in basal conditions in neurons *in vitro*. In contrast, this drug modulates Ca^{2+} entry into the cytosol through VGCCs during membrane depolarization with KCl or NMDA receptor stimulation, which in the latter, prevents cells from excitotoxic mitochondrial Ca^{2+} overload and neuronal death. Thus, our results provide evidence of a new NCLX-independent neuroprotective mechanism of CGP37157 and calls into question its specificity as a NCLX inhibitor in experimental paradigms that involve neuronal depolarization and cytosolic Ca^{2+} overload.

Expression of NCLX in primary cultured neurons. Little is known about the expression and distribution of NCLX in the

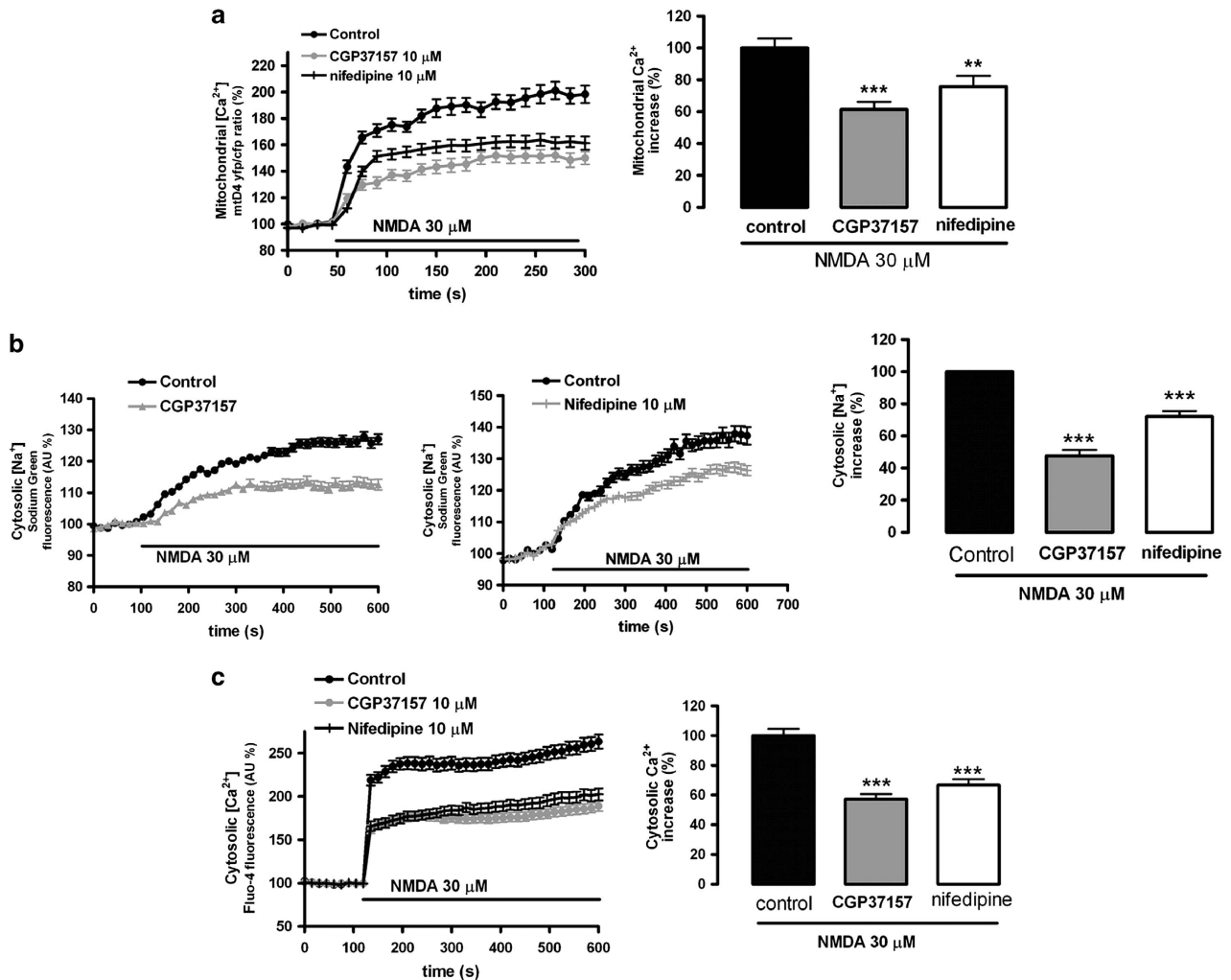


Figure 4 CGP37157 reduces NMDA-induced cytosolic and mitochondrial Ca^{2+} overloads by regulation of VGCCs. (a) Both CGP37157 and nifedipine reduce NMDA-induced mitochondrial Ca^{2+} overload in neurons. NMDA (30 μM) was added as indicated and mitochondrial Ca^{2+} levels monitored in the absence ($n=33$) or presence of CGP37157 (10 μM , 1 h, $n=42$) and nifedipine (10 μM , 30 min, $n=41$). Traces represent the time course of normalized yfp/cfp average ratios \pm S.E.M. of cells from at least three independent culture/experiments. For statistical analysis, normalized average \pm S.E.M. of the area under curve was calculated. $**P<0.01$, $***P<0.001$ compared with control cells (NMDA alone); Student's *t*-test. (b) CGP37157 and nifedipine modulate NMDA-induced Na^+ entry to the cytosol. Cells loaded with Sodium Green dye were exposed to 30 μM of NMDA ($n=99$) as indicated and the effects of CGP37157 ($n=83$) and nifedipine ($n=68$) analyzed. Traces represent the time course of normalized means \pm S.E.M. recorded from single neurons. For statistical analysis normalized average \pm S.E.M. of the area under curve was calculated. $***P<0.001$ compared with control cells (NMDA alone); Student's *t*-test. (c) CGP37157 regulates NMDA-induced cytosolic Ca^{2+} overload similarly to VGCC blocker nifedipine. Fluo-4-loaded neurons were exposed to 30 μM of NMDA in the absence ($n=91$) or presence of CGP37157 (10 μM , 1 h, $n=102$) or nifedipine (10 μM , 30 min, $n=68$) and cytosolic Ca^{2+} loads quantified. Traces represent normalized means \pm S.E.M. from at least three independent cultures/experiments. For statistical analysis normalized average \pm S.E.M. of the area under curve was calculated. $***P<0.001$ compared with control cells (NMDA alone); Student's *t*-test

different cell types of the CNS. Yet, a recent study showed that astrocytes express the NCLX 50 kDa form and the 100 kDa dimer in mitochondria and that it has a major role in intracellular signaling, gliotransmission and proliferation.²⁴ In cortical neurons *in vitro*, we found NCLX is also expressed in mitochondria, as assessed by double labeling immunofluorescence. In addition, immunoblotting revealed the presence of both the 50- and 70-kDa isoforms, which suggests a differential expression of NCLX species in the various cell types of the CNS. This raises the intriguing question as to whether the two alternatively spliced isoforms may subserve diverse functional properties. In addition, some of the NCLX staining does not colocalize with red mitochondria in DsRed positive cells, indicating that NCLX might be expressed in

other compartments different to mitochondria in neurons, as described before in HEK-293 cells.¹⁷

Effects of CGP37157 on neuronal Ca^{2+} homeostasis.

The benzothiazepine CGP37157 inhibits the mitochondrial $\text{Na}^+/\text{Ca}^{2+}$ exchange with a 10 to 20-fold higher affinity than other analogs like diltiazem and clonazepam³¹ and to date, it remains as the only effective and relatively specific drug to target the NCLX.¹⁸ Thus, CGP37157 at 10 and 20 μM inhibits mitochondrial Ca^{2+} efflux following an ATP stimulus in SHSY-5Y cells⁴ and astrocytes.²⁴ Our results in resting neurons show that CGP37157 at that concentration causes a concomitant increase and decrease in intracellular Na^+ and Ca^{2+} , which is consistent with an inhibition of the NCLX.

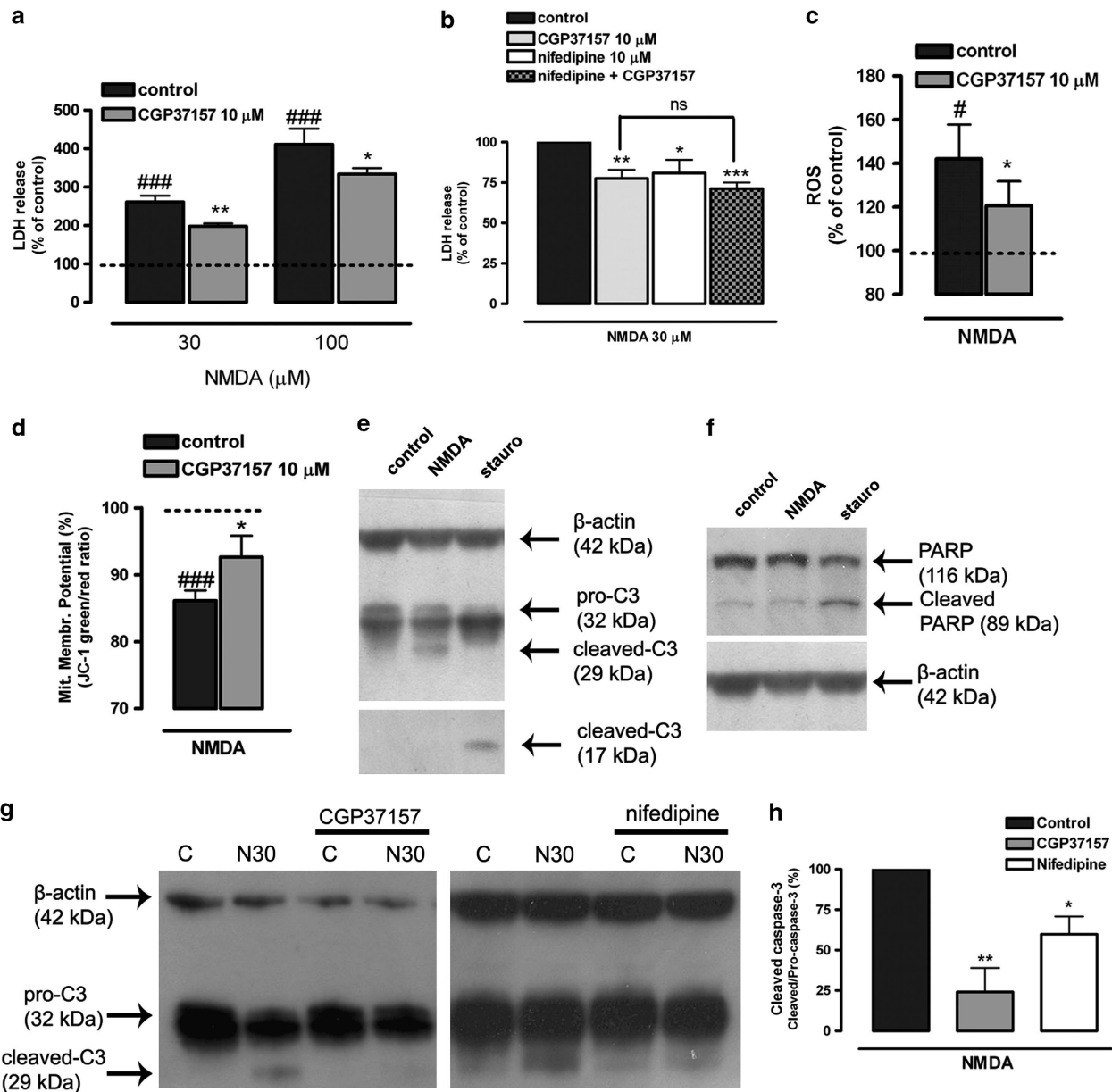


Figure 5 CGP37157 protects neurons from excitotoxicity by attenuating mitochondrial damage and calpain activity. **(a, b)** NMDA-induced neuronal excitotoxicity is reduced by CGP37157 and nifedipine. **(a)** Neurons were stimulated with increasing concentrations of NMDA (30 and 100 μM) in the presence or absence of CGP37157 (10 μM, 1 h) and LDH release to the extracellular medium was quantified 24 h later ($n = 7$). Data represent means \pm S.E.M. of LDH activity values (arbitrary units) from at least three independent experiments. ### $P < 0.001$ compared with untreated cells; * $P < 0.05$, ** $P < 0.01$ compared with control (NMDA alone), paired Student's t -test. **(b)** Cells were stimulated with NMDA 30 μM in the presence of nifedipine alone (10 μM, 30 min, $n = 6$) or nifedipine together with CGP37157 ($n = 6$) and LDH release quantified as described above. * $P < 0.05$, ** $P < 0.01$, *** $P < 0.001$ compared with control (NMDA alone), paired Student's t -test. **(c)** CGP37157 regulates NMDA-induced oxidative stress. ROS levels were quantified at 30 min after the insult using the CM-H2DCFDA fluorescent probe (30 μM). Data represent means \pm S.E.M. of normalized CM-DCFDA/calcein-AM values of cells from $n = 4$ independent cultures. # $P < 0.05$ compared with untreated cells; * $P < 0.05$ compared with control (NMDA alone), paired Student's t -test. **(d)** CGP37157 attenuates mitochondrial membrane depolarization during excitotoxicity. Cells were stimulated with NMDA (30 μM, 10 min) after the addition of CGP37157 (10 μM, 1 h) and mitochondrial membrane potential was measured using JC-1 fluorescent dye 45 min after NMDA application ($n = 4$). Data represent normalized means \pm S.E.M. of the JC-1 red/green fluorescence ratio. ### $P < 0.001$ compared with untreated cells; * $P < 0.05$ compared with control (NMDA alone), paired Student's t -test. **(e)** NMDA induces m-calpain-mediated caspase-3 cleavage. Cells were exposed to NMDA (30 μM, 30 min) or staurosporine (100 nM, 24 h), and harvested 24 h later for the detection of pro-caspase-3 and its cleavage products by western blot. **(f)** Staurosporine but not NMDA triggers caspase-3-mediated PARP cleavage. Cells were exposed to NMDA (30 μM, 30 min) or staurosporine (100 nM, 24 h) and harvested 24 h later for the detection of PARP and its cleavage product by western blot. **(g and h)** NMDA-induced activation of caspase-3 is diminished in the presence of CGP37157 and nifedipine. **(g)** Cells were exposed to NMDA (30 μM, 30 min) after pre-incubation with CGP37157 and nifedipine and harvested 4 h later for the detection of caspase-3 and its cleavage product by western blot ($n = 4$). **(h)** For the quantification of caspase-3 activation, cleaved/pro-caspase-3 ratio was calculated and normalized to β-actin values. * $P < 0.05$, ** $P < 0.01$ compared with control (NMDA alone), paired Student's t -test

In addition, we provide evidence that CGP37157 inhibits mitochondrial Ca^{2+} efflux after ACh receptor activation in cultured neurons. Interestingly, ACh-induced mitochondrial Ca^{2+} influx was also significantly reduced in the presence of CGP37157, an unexpected effect for a mitochondrial $\text{Na}^+/\text{Ca}^{2+}$ exchanger inhibition that suggest additional interactions for this drug. Indeed, there is some evidence that CGP37157 may inhibit L-type VGCCs in dorsal root ganglion neurons and SH-SY5Y cells^{19,23} and that it directly regulates ER Ca^{2+} uptake and release in striated muscle.²² Because of that, we tested the effects of CGP37157 on VGCCs and found that CGP37157 efficiently blocks high K^+ -induced $[\text{Ca}^{2+}]_i$ increase in neurons, with an efficacy similar to that of the VGCC inhibitor nifedipine. Moreover, we found that depolarization induces a $[\text{Ca}^{2+}]_{mit}$ increase that is reduced as well by CGP37157. Importantly, nifedipine-reduced as well acetylcholine-induced mitochondrial Ca^{2+} transient but not the Ca^{2+} efflux, which confirms that the Ca^{2+} efflux inhibition is a specific effect provided by CGP37157 (data not shown). However, ER Ca^{2+} release values, indicative for ER Ca^{2+} content, suggest that CGP37157 does not contribute to ER store depletion in resting neurons. In turn, the $[\text{Ca}^{2+}]_i$ increase following the thapsigargin-induced initial Ca^{2+} transient was absent in CGP37157-treated neurons, which might be due to a modulation of the store-operated Ca^{2+} entry (SOCE) by NCLX activity, an effect that was recently described in astrocytes.²⁴

CGP37157 modulates NMDA-induced cytosolic and mitochondrial Ca^{2+} overloads. Glutamate excitotoxicity contributes to many brain pathologies such as ischemia and traumatic brain injury via NMDA receptor-mediated Ca^{2+} signaling.³² CGP37157 regulates glutamate-induced cytosolic Ca^{2+} transients by the selective inhibition of the mitochondrial $\text{Na}^+/\text{Ca}^{2+}$ exchanger in neurons,³³ but little is known about how this NCLX inhibitor modulates mitochondrial Ca^{2+} signaling during NMDA receptor-mediated excitotoxicity. Again, we observed that intracellular Ca^{2+} measurements during NMDA application in presence of the CGP37157 were not consistent with a specific inhibition of the NCLX. In agreement with previous observations in hippocampal slices subjected to an Na^+ and Ca^{2+} overload,⁸ we found that CGP37157 reduces significantly the excitotoxic $[\text{Ca}^{2+}]_i$ increase, as expected from an NCLX inhibition. However, we found that $[\text{Ca}^{2+}]_{mit}$ and $[\text{Na}^+]_i$ were reduced as well, indicating that CGP37157 blocks Ca^{2+} entry from the extracellular space rather than inhibiting the mitochondrial $\text{Na}^+/\text{Ca}^{2+}$ exchanger. Indeed, previous studies suggested that CGP37157 does not potentiate neuronal mitochondrial Ca^{2+} uptake during glutamate insults, as evaluated by indirect $[\text{Ca}^{2+}]_{mit}$ analysis.³⁴ In contrast, it was recently described that mitochondrial Ca^{2+} accumulation is increased by CGP37157 as a result of NCLX inhibition during exposure to ATP in astrocytes.²⁴ However, this selective effect of CGP37157 was observed after metabotropic receptor stimulation and thus in conditions that primarily do not involve significant extracellular Ca^{2+} entry.

As CGP37157 blocked VGCCs in neurons, we tested whether these channels contributed to NMDA-induced intracellular Ca^{2+} loads *in vitro*. Nifedipine, like CGP37157,

reduced NMDA-induced cytosolic Ca^{2+} and Na^+ loads, as well as $[\text{Ca}^{2+}]_{mit}$ increase. These data demonstrate the recruitment of VGCCs in NMDA-induced Ca^{2+} signals, and strongly suggest that CGP37157 attenuates cytosolic and mitochondrial Ca^{2+} overload as a consequence of the negative modulation of these channels.

CGP37157 protects neurons from mitochondrial damage and cell death. Mitochondrial Ca^{2+} overload and subsequent mitochondrial membrane potential collapse are critical events in excitotoxic neuronal death,³⁵ and this premise predicts that the inhibition of mitochondrial Ca^{2+} efflux would make cells more vulnerable against an intracellular Ca^{2+} overload. Nevertheless, Nicolau *et al.*⁸ showed that CGP37157 protected hippocampal slices against veratridine-induced Ca^{2+} and Na^+ overload by regulating the oxidative stress and p38 MAPK-linked death pathway. Our results indicate as well that CGP37157 protects cortical neurons against excitotoxicity. CGP37157 reduced NMDA-induced oxidative stress and mitochondrial membrane depolarization, likely by attenuating mitochondrial Ca^{2+} overload. In addition, preventing the $[\text{Ca}^{2+}]_i$ elevation, CGP37157 reduced m-calpain activity, which is involved in NMDAR-mediated neurodegeneration.³⁶ On the other hand, consistent with its regulation of $[\text{Ca}^{2+}]_i$ and $[\text{Ca}^{2+}]_{mit}$ during excitotoxicity, nifedipine was as efficient as CGP37157 in protecting neurons against NMDA-induced neuronal death and the effects of both inhibitors were not additive. Although inhibition of the NCLX may also contribute to neuroprotection through the prevention of the mitochondrial futile Ca^{2+} cycling³⁷ and the modulation of SOCE, we conclude that the neuroprotective effect by CGP37157 during NMDA receptor-mediated excitotoxicity relies mainly on VGCC blockade and the attenuation of intracellular Ca^{2+} overload. Indeed, L-type VGCCs are considered as relevant contributors to excitotoxicity, in particular in mature neurons¹⁵ and late stages of glutamate-mediated injury.¹⁶ The multi-target effect of CGP37157 described here may represent a potential therapeutic strategy in neurological disorders involving excitotoxicity and intracellular Ca^{2+} homeostasis disruption.

Materials and Methods

Animals. All experiments were conducted under the supervision and with the approval of our internal animal ethics committee (University of the Basque Country, UPV/EHU). Animals were handled in accordance with the European Communities Council Directive. All possible efforts were made to minimize animal suffering and the number of animals used.

Reagents and plasmids. Neurobasal medium, B27 supplement, calcein-AM (calcein acetoxymethyl ester), CM-H2DCFDA and JC-1 were purchased from Invitrogen (Barcelona, Spain). NMDA, HBSS, glycine, poly-L-ornithine, thapsigargin and nifedipine were obtained from Sigma (St. Louis, MO, USA). CGP37157 (7-Chloro-5-(2-chlorophenyl)-1,5-dihydro-4,1-benzothiazepin-2(3H)-one) was obtained from Tocris Biosciences (Minneapolis, MN, USA). Cytotox 96 for LDH release quantification was purchased from Promega (Madison, WI, USA).

The plasmid expressing mitochondria-targeted Ca^{2+} indicator (2mtD4cpv) was kindly provided by Roger Tsien (University of California, San Diego, La Jolla, CA, USA). Mitochondrial DsRed expressing plasmid was obtained from Clontech (Takara Bio Inc., Otsu, Japan).

Neuronal primary culture and transfection procedures. Cortical neurons were obtained from the cortical lobes of E18 Sprague-Dawley rat

embryos according to previously described procedures.^{38,39} Neurons were resuspended in B27 Neurobasal medium plus 10% FBS and then seeded onto poly-L-ornithine-coated 48-well plates or glass coverslips (12 mm in diameter) at 1.5×10^5 cells per well. For confocal single-cell imaging experiments, cells were plated onto glass-bottom μ -dishes (Ibidi GmbH, Planegg/Martinsried, Germany). The medium was replaced by serum-free, B27-supplemented Neurobasal medium 24 h later. The cultures were essentially free of astrocytes and microglia and were maintained at 37 °C and 5% CO₂. Cultures were used at 8–9 days *in vitro*.

For transfection of cells, 4×10^6 rat neurons were transfected in suspension before plating with 3 μ g of cDNA using Rat Neuron Nucleofector Kit (Lonza, Basel, Switzerland) according to the manufacturer instructions and plated and maintained as described above.

Immunocytochemistry. For NCLX expression analysis, eight DIV mtDsRed-transfected neurons were fixed with 4% paraformaldehyde for 20 min and permeabilized in 1% BSA, 1% normal serum, 0.05% Triton X-100 in PBS for 30 min. Then, cells were blocked in 10% BSA, 1% normal serum in PBS for 1 h and incubated overnight at 4 °C with anti-NCLX (1 : 500, LifeSpan BioSciences, Seattle, WA, USA) in 1% BSA, 1% normal serum in PBS. After washing with PBS, Alexa Fluor 488-conjugated secondary antibody (1 : 200, Molecular Probes, Barcelona, Spain) was added for 1 h. Finally, coverslips were washed in PBS and mounted using ProLong Gold mounting medium (Invitrogen). Controls without a primary antibody showed no staining. Images were acquired by a TCS SP8X confocal microscope (Leica, Wetzlar, Germany) and deconvolution and fluorescence intensity plot were performed by Huygens software (SVI, Hilversum, The Netherlands). For colocalization quantification, neuronal bodies of several cells were selected as ROIs and Overlap Coefficient was calculated using Leica LAS AF software.

Western blotting. Cells (triplicates of 1.5×10^4) were washed with PBS and harvested in 50 μ l of ice-cold electrophoresis sample buffer. Lysates were boiled for 10 min, separated by electrophoresis using Criterion TGX Precast 12% gels and transferred to Trans-Blot Turbo Midi Nitrocellulose Transfer Packs (Bio-Rad, Hercules, CA, USA). For immunoblotting, membranes were blocked in 5% skimmed milk, 5% serum in TBST and proteins detected by specific primary antibodies in 5% BSA in TBST overnight at 4 °C: anti-NCLX (1 : 1000; LifeSpan Biosciences); anti-caspase-3 (1 : 1000, Santa Cruz Biotechnology, Dallas, TX, USA); anti-PARP (1 : 1000, Cell Signaling, Danvers, MA, USA). After washing, membranes were incubated with horseradish peroxidase-conjugated secondary antibodies (1 : 2000, Sigma) in 5% skimmed milk, 1% normal serum in TTBS for 2 h RT and developed using enhanced chemiluminescence according to the manufacturer's instructions (Super Signal West Dura, Pierce, Rockford, IL, USA). In quantitative immunoblotting experiments, signals were quantified using Image-J software (NIH, Bethesda, MD, USA) and values were normalized to β -actin signal and provided as the mean \pm S.E.M. of at least three independent experiments.

Cytosolic Na⁺ and Ca²⁺ imaging. For [Ca²⁺]_i measurements, neurons were loaded with Fluo-4 AM (1 μ M; Molecular Probes, Invitrogen) in Ca²⁺ and Mg²⁺ free HBSS containing 20 mM HEPES, pH 7.4, 10 mM glucose, 10 μ M glycine and 2.6 mM CaCl₂ (incubation buffer) for 30 min at 37 °C followed by 20 min wash to allow de-esterification. For cytosolic Na⁺ imaging, cells were loaded with Sodium Green tetraacetate (5 μ M, 1 h) and pluronic acid (0.025% w/v, Invitrogen) followed by 30 min wash in incubation buffer. Images were acquired through a 63X objective by inverted LCS SP2 confocal microscope (Leica) at an acquisition rate of one frame/15 s for 5 or 10 min depending on the experiment. Both Fluo-4 AM- and Sodium Green-loaded cells were excited at 488 nm. For data analysis, a homogeneous population of 15–25 cells was selected in the field of view and neuronal somata selected as ROIs. Background values were always subtracted and data are expressed as $F/F_0 \pm$ S.E.M. (%) in which F represents the fluorescence value for a given time point and F_0 represents the mean of the resting level fluorescence.

Mitochondrial Ca²⁺ imaging. Neurons transfected with mitochondria-targeted 2mtD4cpv Ca²⁺ indicator⁴⁰ were transferred to incubation buffer (see above) and imaged by a TCS SP8X confocal microscope (Leica). Cells were excited at 458 nm and cfp and yfp emission acquired for FRET ratio quantification at an acquisition rate of one frame/15 s for 5 or 10 min depending on the experiment. For data analysis, a homogeneous population of 5–12 cells was selected in the field of view and neuronal somata selected as ROIs. Background values were always subtracted and data are expressed as $R/R_0 \pm$ S.E.M. (%) in which R represents the yfp/cfp fluorescence ratio for a given time point and R_0 represents the mean of the resting FRET ratio.

Neuronal toxicity assays. Cell toxicity assays were performed as described previously⁴¹ with modifications. Neurons were exposed to NMDA in HBSS (free of Ca²⁺ and Mg²⁺) containing 2.6 mM CaCl₂, 10 mM glucose and 10 μ M glycine for 10 or 30 min at 37 °C, depending on the experiment. Antagonists were present before and during the excitotoxic insult and cell viability was assessed 24 h later using Citotox 96 colorimetric assay (Promega). All experiments were performed in quadruplicate and the values provided are the normalized mean \pm S.E.M. of at least three independent experiments.

Intracellular reactive oxygen species (ROS) and mitochondrial membrane potential measurements. Neurons were stimulated with NMDA for 10 min in the absence or presence of antagonists and loaded with 5-(and 6)-chloromethyl-2'-7'-dichlorodihydrofluorescein diacetate acetyl ester (CM-H₂DCFDA) for 30 min for the measurement of generated ROS. Calcein-AM (1 μ M) was used to quantify the number of cells within the reading field and fluorescence was measured as described previously.⁴² For quantification of mitochondrial membrane potential, cells were loaded 30 min after the excitotoxic stimulus with JC-1 dye for 15 min and red/green fluorescence ratio was measured. All experiments were performed in quadruplicate and the values provided are the normalized mean \pm S.E.M. of at least three independent experiments.

Data analysis. All data are expressed as mean \pm S.E.M. (n), where n refers to the number of cultures assayed, each obtained from a different group of animals. In single cell Ca²⁺ imaging experiments, n refers to number of cells recorded from at least three independent cultures obtained from different groups of animals. For statistical analysis of the [Ca²⁺]_i and [Na⁺]_i increase or accumulation, basal line-extracted area under curve was calculated from single cell imaging time-lapses. Ca²⁺ efflux was represented as the declining slope of the [Ca²⁺]_i time course as described before.⁴ Statistical analysis was carried out with Student's t -test and significance was determined at $P < 0.05$.

Conflict of Interest

The authors declare no conflict of interest.

Acknowledgements. This work was supported by CIBERNED, MINECO, Gobierno Vasco and the University of Pais Vasco. We thank Dr. Szabadkai and Dr. Duchon at the University College of London for their help in setting up the mitochondrial Ca²⁺ imaging approaches.

1. Nicholls DG. Mitochondrial calcium function and dysfunction in the central nervous system. *Biochim Biophys Acta* 2009; **1787**: 1416–1424.
2. Drago I, Pizzo P, Pozzan T. After half a century mitochondrial calcium in- and efflux machineries reveal themselves. *EMBO J* 2011; **30**: 4119–4125.
3. Pizzo P, Drago I, Filadi R, Pozzan T. Mitochondrial Ca²⁺ homeostasis: mechanism, role, and tissue specificities. *PLoS Arch* 2012; **464**: 3–17.
4. Patly R, Silverman WF, Hershinkel M, Caporale T, Sensi SL, Parnis J *et al*. NCLX is an essential component of mitochondrial Na⁺/Ca²⁺ exchange. *Proc Natl Acad Sci USA* 2010; **107**: 436–441.
5. Cox DA, Conforti L, Sperelakis N, Matlib MA. Selectivity of inhibition of Na(+)-Ca2+ exchange of heart mitochondria by benzothiazepine CGP-37157. *J Cardiovasc Pharmacol* 1993; **21**: 595–599.
6. Patly R, Sekler I. The mitochondrial Na⁺/Ca²⁺ exchanger. *Cell Calcium* 2012; **52**: 9–15.
7. Castaldo P, Cataldi M, Magi S, Lariccia V, Arcangeli S, Amoroso S. Role of the mitochondrial sodium/calcium exchanger in neuronal physiology and in the pathogenesis of neurological diseases. *Prog Neurobiol* 2009; **87**: 58–79.
8. Nicolau SM, Egea J, López MG, García AG. Mitochondrial Na⁺/Ca²⁺ exchanger, a new target for neuroprotection in rat hippocampal slices. *Biochem Biophys Res Commun* 2010; **400**: 140–144.
9. Gandhi S, Wood-kaczmar A, Yao Z, Plun-favreau H, Deas E, Klupsch K *et al*. PINK1-associated Parkinson's disease is caused by neuronal vulnerability to calcium-induced cell death. *Molecular Cell* 2009; **33**: 627–638.
10. Choi DW. Excitotoxic cell death. *J Neurobiol* 1992; **23**: 1261–1276.
11. Stout AK, Raphael HM, Kanterewicz BI, Klann E, Reynolds LJ. Glutamate-induced neuron death requires mitochondrial calcium uptake. *Nat Neurosci* 1998; **1**: 366–373.
12. Stanika RI, Pivovarova NB, Brantner CA, Watts CA, Winters CA, Andrews SB. Coupling diverse routes of calcium entry to mitochondrial dysfunction and glutamate excitotoxicity. *Proc Natl Acad Sci USA* 2009; **106**: 9854–9859.
13. Starkov AA, Chinopoulos C, Fiskum G. Mitochondrial calcium and oxidative stress as mediators of ischemic brain injury. *Cell Calcium* 2004; **36**: 257–264.
14. Wang KK. Calpain and caspase: can you tell the difference? *Trends Neurosci* 2000; **23**: 20–26.

15. Brewer LD, Thibault O, Staton J, Thibault V, Rogers JT, Garcia-Ramos G *et al*. Increased vulnerability of hippocampal neurons with age in culture: temporal association with increases in NMDA receptor current, NR2A subunit expression and recruitment of L-type calcium channels. *Brain Res* 2007; **1151**: 20–31.
16. Prehn JH, Lippert K, Kriegstein J. Are NMDA or AMPA/kainate receptor antagonists more efficacious in the delayed treatment of excitotoxic neuronal injury? *Eur J Pharmacol* 1995; **292**: 179–189.
17. Cai X, Lytton J. Molecular cloning of a sixth member of the K⁺-dependent Na⁺/Ca²⁺ exchanger gene family, NCKX6. *J Biol Chem* 2004; **279**: 5867–5876.
18. Csordás G, Várnai P, Golenár T, Sheu SS, Hajnóczky G. Calcium transport across the inner mitochondrial membrane: molecular mechanisms and pharmacology. *Mol Cell Endocrinol* 2012; **353**: 109–113.
19. Baron KT, Thayer SA. CGP37157 modulates mitochondrial Ca²⁺ homeostasis in cultured rat dorsal root ganglion neurons. *Eur J Pharmacol* 1997; **340**: 295–300.
20. Luciani DS, Ao P, Hu X, Warnock GL, Johnson JD. Voltage-gated Ca²⁺ influx and insulin secretion in human and mouse beta-cells are impaired by the mitochondrial Na⁺/Ca²⁺ exchange inhibitor CGP-37157. *Eur J Pharmacol* 2007; **576**: 18–25.
21. Lee B, Miles PD, Vargas L, Luan P, Glasco S, Kushnareva Y *et al*. Inhibition of mitochondrial Na⁺-Ca²⁺ exchanger increases mitochondrial metabolism and potentiates glucose-stimulated insulin secretion in rat pancreatic islets. *Diabetes* 2003; **52**: 965–973.
22. Neumann JT, Diaz-sylvester PL, Fleischer S, Copello JA. CGP-37157 inhibits the sarcoplasmic reticulum Ca²⁺ ATPase and activates ryanodine receptor channels in striated muscle. *Mol Pharmacol* 2011; **79**: 141–147.
23. González-Lafuente L, Egea J, León R, Martínez-Sanz FJ, Monjas L, Perez C *et al*. Benzothiazepine CGP37157 and its isosteric 2'-methyl analogue provide neuroprotection and block cell calcium entry. *ACS Chem Neurosci* 2012; **3**: 519–529.
24. Parnis J, Montana V, Delgado-Martinez I, Matyash V, Parpura V, Kettenmann H *et al*. Mitochondrial exchanger NCLX plays a major role in the intracellular Ca²⁺ signaling, gliotransmission, and proliferation of astrocytes. *J Neurosci* 2013; **33**: 7206–7219.
25. Peng TI, Greenamyre JT. Privileged access to mitochondria of calcium influx through N-methyl-D-aspartate receptors. *Mol Pharmacol* 1998; **53**: 974–980.
26. Ruiz A, Matute C, Alberdi E. Endoplasmic reticulum Ca²⁺ release through ryanodine and IP(3) receptors contributes to neuronal excitotoxicity. *Cell Calcium* 2009; **46**: 273–281.
27. Blomgren K, Zhu C, Wang X, Karlsson JO, Leverin AL, Bahr BA *et al*. Synergistic activation of caspase-3 by m-calpain after neonatal hypoxia-ischemia: a mechanism of "pathological apoptosis"? *J Biol Chem* 2001; **276**: 10191–10198.
28. Lankiewicz S. Activation of calpain I converts excitotoxic neuron death into a caspase-independent cell death. *J Biol Chem* 2000; **275**: 17064–17071.
29. Zhang C, Shen W, Zhang G. N-methyl-D-aspartate receptor and L-type voltage-gated Ca(2+) channel antagonists suppress the release of cytochrome c and the expression of procaspase-3 in rat hippocampus after global brain ischemia. *Neurosci Lett* 2002; **328**: 265–268.
30. Zhang Y, Lipton P. Cytosolic Ca²⁺ changes during in vitro ischemia in rat hippocampal slices: major roles for glutamate and Na⁺-dependent Ca²⁺ release from mitochondria. *J Neurosci* 1999; **19**: 3307–3315.
31. Chiesi M, Schwaller R, Eichenberger K. Structural dependency of the inhibitory action of benzodiazepines and related compounds on the mitochondrial Na⁺-Ca²⁺ exchanger. *Biochem Pharmacol* 1988; **37**: 4399–4403.
32. Arundine M, Tymianski M. Molecular mechanisms of glutamate-dependent neurodegeneration in ischemia and traumatic brain injury. *Cell Mol Life Sci* 2004; **61**: 657–668.
33. White RJ, Reynolds IJ. Mitochondria accumulate Ca²⁺ following intense glutamate stimulation of cultured rat forebrain neurones. *J Physiol* 1997; **498**(Pt 1): 31–47.
34. Scanlon JM, Brocard JB, Stout AK, Reynolds IJ. Pharmacological investigation of mitochondrial Ca²⁺ transport in central neurons: studies with CGP-37157, an inhibitor of the mitochondrial Na⁺-Ca²⁺ exchanger. *Cell Calcium* 2000; **28**: 317–327.
35. Duchen MR. Mitochondria and calcium: from cell signalling to cell death. *J Physiol* 2000; **529**(Pt 1): 57–68.
36. Wang Y, Briz V, Chishti A, Bi X, Baudry M. Distinct roles for μ -calpain and m-calpain in synaptic NMDAR-mediated neuroprotection and extrasynaptic NMDAR-mediated neurodegeneration. *J Neurosci* 2013; **33**: 18880–18892.
37. Fernández-Morales JC, Arranz-Tagarro JA, Calvo-Gallardo E, Maroto M, Padín JF, García AG. Stabilizers of neuronal and mitochondrial calcium cycling as a strategy for developing a medicine for Alzheimer's disease. *ACS Chem Neurosci* 2012; **3**: 873–883.
38. Larm JA, Cheung NS, Beart PM. (S)-5-fluorowillardine-mediated neurotoxicity in cultured murine cortical neurones occurs via AMPA and kainate receptors. *Eur J Pharmacol* 1996; **314**: 249–254.
39. Cheung NS, Pascoe CJ, Giardina SF, John CA, Beart PM. Micromolar L-glutamate induces extensive apoptosis in an apoptotic-necrotic continuum of insult-dependent, excitotoxic injury in cultured cortical neurones. *Neuropharmacology* 1998; **37**: 1419–1429.
40. Palmer AE, Giacomello M, Kortemme T, Hires SA, Lev-Ram V, Baker D *et al*. Ca²⁺ indicators based on computationally redesigned calmodulin-peptide pairs. *Chem Biol* 2006; **13**: 521–530.
41. Schubert D, Kimura H, Maher P. Growth factors and vitamin E modify neuronal glutamate toxicity. *Proc Natl Acad Sci USA* 1992; **89**: 8264–8267.
42. Campos-Esparza MR, Sánchez-Gómez MV, Matute C. Molecular mechanisms of neuroprotection by two natural antioxidant polyphenols. *Cell Calcium* 2009; **45**: 358–368.



Cell Death and Disease is an open-access journal published by Nature Publishing Group. This work is licensed under a Creative Commons Attribution-NonCommercial-ShareAlike 3.0 Unported License. The images or other third party material in this article are included in the article's Creative Commons license, unless indicated otherwise in the credit line; if the material is not included under the Creative Commons license, users will need to obtain permission from the license holder to reproduce the material. To view a copy of this license, visit <http://creativecommons.org/licenses/by-nc-sa/3.0/>